Longitudinal dynamics of the human B cell response to the yellow fever 17D vaccine

Anna Z. Wec[a], Denise Haslwanter[b], Yasmina N. Abdiche[c], Laila Shehata[a,1], Nuria Pedreño-Lopez[d], Crystal L. Moyer[e], Zachary A. Bornholdt[e], Asparouh Lilov[a], Juergen H. Nett[a], Rohit K. Jangra[b], Michael Brown[a], David I. Watkins[d], Clas Ahlm[f], Mattias N. Forsell[f], Félix A. Rey[g], Giovanna Barba-Spaeth[g], Kartik Chandran[b], and Laura M. Walker[a,2]

[a]Adimab, LLC, Lebanon, NH 03766; [b]Department of Microbiology and Immunology, Albert Einstein College of Medicine, Bronx, NY 10461; [c]Carterra Inc., Salt Lake City, UT 84103; [d]Department of Pathology, University of Miami, Miami, FL 33146; [e]Mapp Biopharmaceutical, Inc., San Diego, CA 92121; [f]Division of Infection & Immunology, Department of Clinical Microbiology, Umeå University, 90187 Umeå, Sweden; and [g]Structural Virology Unit, CNRS UMR 3569, Virology Department, Institut Pasteur, 75015 Paris, France

Edited by Adolfo Garcia-Sastre, Icahn School of Medicine at Mount Sinai, New York, NY, and approved February 12, 2020 (received for review December 9, 2019)

A comprehensive understanding of the development and evolution of human B cell responses induced by pathogen exposure will facilitate the design of next-generation vaccines. Here, we utilized a high-throughput single B cell cloning technology to longitudinally track the human B cell response to the yellow fever virus 17D (YFV-17D) vaccine. The early memory B cell (MBC) response was mediated by both classical immunoglobulin M (IgM) (IgM^+CD27^+) and switched immunoglobulin ($swIg^+$) MBC populations; however, classical IgM MBCs waned rapidly, whereas $swIg^+$ and atypical IgM^+ and IgD^+ MBCs were stable over time. Affinity maturation continued for 6 to 9 mo following vaccination, providing evidence for the persistence of germinal center activity long after the period of active viral replication in peripheral blood. Finally, a substantial fraction of the neutralizing antibody response was mediated by public clones that recognize a fusion loop-proximal antigenic site within domain II of the viral envelope glycoprotein. Overall, our findings provide a framework for understanding the dynamics and complexity of human B cell responses elicited by infection and vaccination.

antiviral vaccination | antibody responses | yellow fever virus | monoclonal antibody | B cell memory

Memory B cells (MBCs) formed in response to infection and vaccination provide protection against the consequences of reexposure to the same pathogen. These cells can differentiate into antibody-secreting cells to provide an immediate source of serum antibody (Ab) or they can enter germinal centers (GCs) to rediversify their B cell receptors (BCRs) in response to evolving or antigenically related pathogens (1). Over the past decade, numerous studies have shown that the MBC compartment in both humans and mice is highly heterogenous (2). In humans, both switched immunoglobulin ($swIg^+$) and immunoglobulin M (IgM^+) memory cells have been described, as well as "atypical" MBCs that express FCRL4 or FCRL5 and/or lack expression of the canonical MBC surface marker CD27 (2, 3). Various activated B cell subsets, which appear transiently after infection or vaccination, have also been reported (4–6). In mice, MBCs can be subcategorized based on their expression of Ig isotype as well as other surface markers, such as CD80, PD-L2, and CD73 (2, 7). Interestingly, recent studies have shown that murine IgM^+ MBCs formed in response to immunization with model proteins are abundant and stable over time, whereas the longevity of antigen-specific $swIg^+$ MBCs appears to be dependent on the frequency of high-avidity germline-encoded BCRs in the naïve B cell repertoire (8–10). Although these studies have provided important insights into the hierarchy of murine IgM^+ and $swIg^+$ MBC populations induced by nonreplicating antigens, it remains unclear whether, and how, these findings will translate to human MBC responses induced by infection or vaccination. Furthermore, the relative contribution of different MBC subsets to the human B cell response to pathogen exposure, and if/how these subsets change over time, remains to be elucidated.

Due to the high level of protection afforded by the live-attenuated yellow fever virus 17D (YFV-17D) vaccine—reported to be primarily mediated by neutralizing antibodies (nAbs) targeting the YFV E protein (11)—we sought to gain a comprehensive view of the human YFV E-specific B cell response underlying this efficacy. Importantly, despite its success, our knowledge of the human B cell response to the YFV-17D vaccine remains limited to studies of human sera and a handful of YFV E-specific human monoclonal Abs (mAbs). Recent serum depletion studies have shown that a large fraction of the YFV E-specific serum Ab response is mediated by Abs targeting domain I (DI) and/or domain II (DII) of the E protein, whereas Abs targeting domain III (DIII) are absent or present at very low titers (12). Correspondingly, the six YFV E-specific human

Significance

The yellow fever virus 17D (YFV-17D) vaccine is one of the safest and most effective vaccines ever developed and is widely considered to be the "gold standard" of antiviral vaccination. Despite its success, remarkably little is known about the human B cell response induced by YFV-17D and the specificities and functional activities of the antibodies encoded by these B cells. Here we report the molecular characterization of the complexity, dynamics, and evolution of this response at the single-cell level. Our work provides key insights into the B cell response underlying the efficacy of the YFV-17D vaccine, which may facilitate the design of vaccines for more refractory pathogens, such as malaria and HIV.

Author contributions: A.Z.W., Y.N.A., A.L., and L.M.W. designed research; A.Z.W., D.H., Y.N.A., L.S., N.P.-L., A.L., and R.K.J. performed research; D.H., N.P.-L., C.L.M., Z.A.B., J.H.N., R.K.J., M.B., D.I.W., C.A., M.N.F., F.A.R., G.B.-S., and K.C. contributed new reagents/analytic tools; A.Z.W., D.H., Y.N.A., L.S., N.P.-L., A.L., M.B., K.C., and L.M.W. analyzed data; and A.Z.W. and L.M.W. wrote the paper.

Competing interest statement: A.Z.W., L.S., A.L., J.H.N., M.B., and L.M.W. are employees and equity holders in Adimab LLC. C.L.M. and Z.A.B. are employees of and shareholders in Mapp Biopharmaceutical, Inc.

This article is a PNAS Direct Submission.

Data deposition: The sequences of neutralizing antibodies isolated in this study have been deposited in the GenBank database, https://www.ncbi.nlm.nih.gov/genbank (accession nos. MN993290–MN993593).

[1]Present address: Department of Immunology, University of Washington School of Medicine, Seattle, WA 98195.

[2]To whom correspondence may be addressed. Email: laura.walker@adimab.com.

This article contains supporting information online at https://www.pnas.org/lookup/suppl/doi:10.1073/pnas.1921388117/-/DCSupplemental.

First published March 9, 2020.

mAbs described to date target overlapping epitopes within DII of the E protein (13, 14).

To longitudinally track the development and evolution of the human B cell response induced by the YFV-17D vaccine, we isolated and characterized hundreds of YFV E-specific mAbs from two flavivirus-naïve donors at multiple time points following YFV-17D vaccination, spanning the course of 360 d. Here we present an analysis of the kinetics, dynamics, and heterogeneity of this B cell response, as well as an in-depth characterization of the mAbs encoded by these B cells. Overall, the results provide a global view of the human MBC response to a highly successful vaccine and may inform the development of vaccines against refractory pathogens, such as malaria and HIV.

Results

Study Design. To study the evolution of the human B cell response to YFV-17D, we immunized two healthy donors with the YFV-17D Stamaril vaccine and collected blood samples at days 10, 14, 28, 90, 180, 270, and 360 postvaccination (*SI Appendix*, Fig. S1*A* and Table S1). Neither of the YFV-17D vaccinees had a history of YFV infection or vaccination, and correspondingly the prevaccination sera from both donors showed no detectable binding reactivity to YFV-17D viral particles or recombinant YFV E or NS1 proteins (*SI Appendix*, Fig. S1 *B–D*). Furthermore, neither prevaccination serum showed detectable neutralizing activity against YFV-17D (*SI Appendix*, Fig. S1*E*). Since YFV is antigenically related to other flaviviruses, we also confirmed that the prevaccination sera from both donors lacked reactivity with E and NS1 proteins from commonly circulating flaviviruses (dengue virus serotypes 1 through 4 [DENV1-4], Japanese encephalitis virus [JEV], tick-borne encephalitis virus, West Nile virus [WNV], and Zika virus [ZIKV]) (*SI Appendix*, Fig. S1 *C* and *D*). Hence, both donors were likely flavivirus-naïve at the time of vaccination. The IgG and IgM serum kinetics following vaccination also supported primary exposure (*SI Appendix*, Fig. S1*F*). Consistent with prior studies (15, 16), serum neutralizing activity against YFV-17D appeared in both donors by day 10 postvaccination and persisted through the course of the study (*SI Appendix*, Fig. S1 *E* and *G*).

Primary YFV-17D Vaccination Induces Highly Mutated Plasmablast Responses in Flavivirus-Naïve Donors. Since previous studies have shown that plasmablasts (PBs) appear transiently in peripheral blood ~10 to 14 d following YFV-17D vaccination (17), we monitored PB responses in both donors on day 10 and 14 postvaccination. In both donors, expanded PB populations that were ~10- to 20-fold over prevaccination levels were observed at both time points (Fig. 1*A* and *SI Appendix*, Fig. S2).

To further characterize the PB response to YFV-17D, we single-cell-sorted ~600 PBs from both donors and amplified the

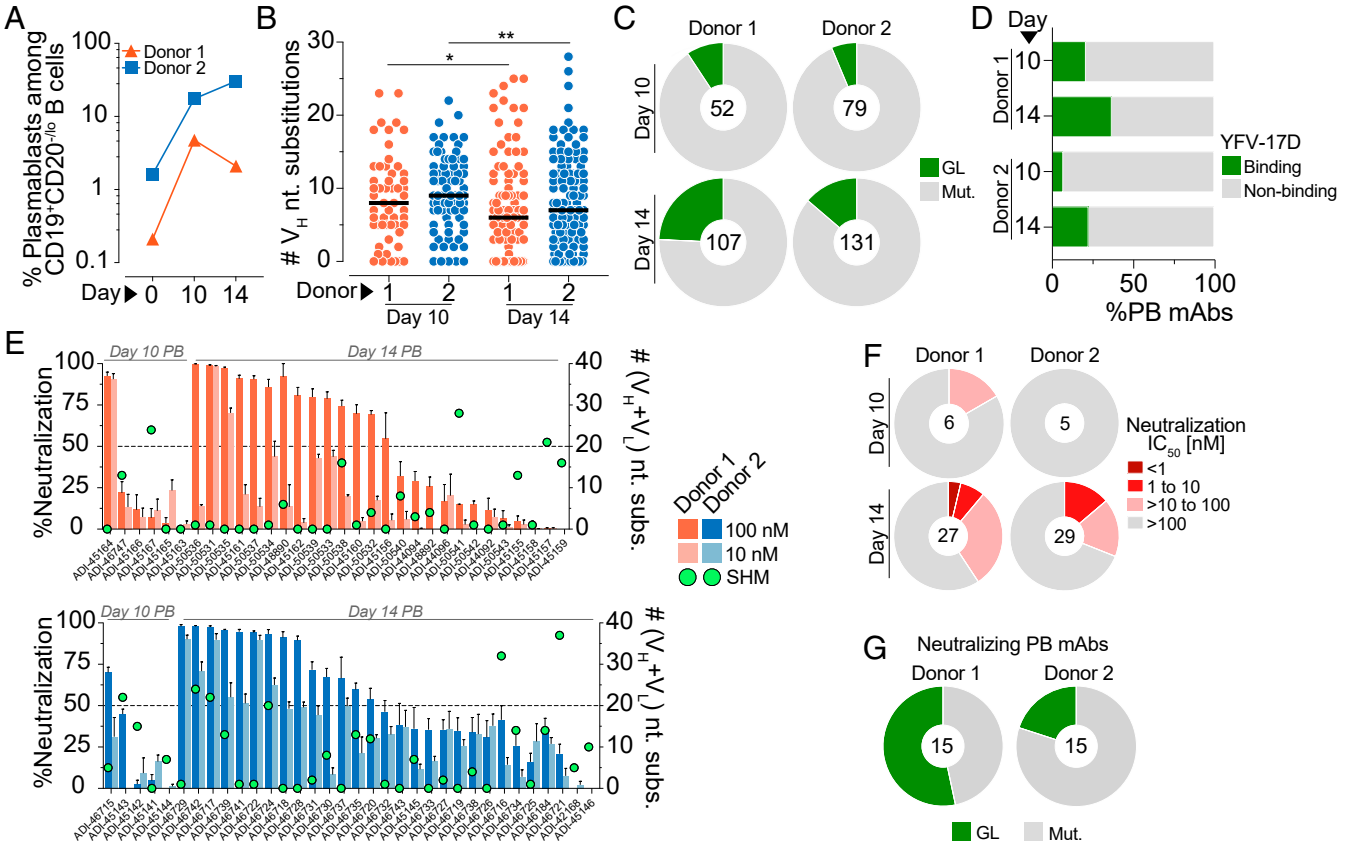

Fig. 1. Molecular characterization of YFV-17D–induced PB responses. (*A*) Frequency of PBs among circulating $CD19^+CD20^{-/lo}$ B cells at days 0, 10, and 14 postvaccination. (*B*) SHM loads of mAbs isolated from day 10 and day 14 PBs. Black bars indicate medians. (*C*) Proportion of mAbs isolated from day 10 and day 14 PBs that contain somatic mutations. (*D*) Percentage of PB-derived mAbs that showed detectable ELISA binding reactivity to whole YFV-17D particles. (*E*) Neutralizing activities of PB-derived mAbs against YFV-17D at 100 nM and 10 nM concentrations. Green dots indicate the number of nucleotide substitutions in $V_H + V_L$ for each mAb. (*F*) Proportion of YFV-17D binding mAbs with the indicated neutralization IC_{50}s. MAbs that displayed <50% neutralization at 100 nM in the preliminary screen are included in the IC_{50} >100 nM group. (*G*) Proportion of PB-derived nAbs (defined as Abs displaying >50% neutralization at 100 nM) that contain somatic mutations. Statistical comparisons were made using the Mann–Whitney *U* test (**$P < 0.01$, *$P < 0.05$). nt, nucleotide; n.n., nonneutralizing; GL, germline; Mut., mutated; V_H, variable region of the heavy chain; IC_{50}, half-maximal inhibitory concentration.

corresponding Ab heavy- and light-chain variable (V_H and V_L) genes by single-cell PCR. One hundred sixty-one and 210 natively paired mAbs were cloned from donors 1 and 2, respectively, and expressed as full-length IgGs in an engineered strain of *Saccharomyces cerevisiae* (18). Sequence analysis showed that the PB responses were highly diverse in both donors, with only about 15% of clones belonging to expanded clonal lineages (*SI Appendix*, Fig. S3). Unexpectedly, a large fraction of the PB-derived mAbs from both donors contained high levels of somatic hypermutation (SHM), suggesting either efficient recruitment of preexisting MBCs into the PB response or the early onset of affinity maturation within GC reactions or at extrafollicular sites (19) (Fig. 1*B*). We also expanded this analysis to include two additional flavivirus-naïve donors and observed similar results (*SI Appendix*, Fig. S4). In three out of four donors, the median level of SHM in the PB-derived mAbs was significantly higher on day 10 than on day 14 (Fig. 1*B* and *SI Appendix*, Fig. S4). Correspondingly, a larger proportion of mAbs cloned from day 14 PBs lacked SHM, suggesting an increased recruitment of cells from the naïve B cell compartment at this time point (Fig. 1*C*). To analyze whether the somatic mutations in the PB-derived mAbs contribute to binding activity, we generated inferred unmutated common ancestor (UCA) mAbs from three somatically mutated PB clones and measured their binding affinities to a recombinant YFV E protein. In all three cases, the UCA mAbs showed substantially reduced binding affinities compared to the mature mAbs, suggesting that somatic mutations in the PB mAbs are important for recognition of YFV E (*SI Appendix*, Fig. S5).

We next tested the PB-derived mAbs for binding reactivity to YFV-17D particles using a sandwich enzyme-linked immunosorbent assay (ELISA) (Fig. 1*D* and *SI Appendix*, Fig. S6*A*). The frequency of YFV-17D binding mAbs isolated from day 10 and 14 PBs ranged from 6 to 37%, which is substantially lower than the percentage of antigen-specific mAbs recovered from PBs induced by influenza vaccination or secondary DENV infection (20, 21). The low proportion of YFV-17D–reactive clones may be due to promiscuous B cell activation (19) or low binding affinity of the PB-derived mAbs or because the PB responses were primarily directed against other viral antigens not tested in this study (e.g., viral core proteins). Notably, the binding and nonbinding populations contained a similar proportion of polyreactive clones, with ∼10 to 20% of PB-derived mAbs showing some degree of polyreactivity (*SI Appendix*, Fig. S6*B*). Thus, it is unlikely that the nonbinding PB population originates from nonspecifically activated, polyreactive B cell clones. Furthermore, the mAbs that failed to bind YFV-17D by ELISA also showed little to no binding to a recombinant YFV E protein in a biolayer interferometry (BLI) assay using an avid binding orientation, indicating the lack of detectable binding to YFV-17D particles by ELISA is likely not due to low affinity or assay format (*SI Appendix*, Fig. S6*C*). Despite the low frequency of YFV-specific clones, we recovered 33 and 34 YFV-17D binding mAbs from the expanded PB populations in donors 1 and 2, respectively. The SHM loads of the binding mAbs were similar to those observed in the total PB population (Fig. 1*B* and *SI Appendix*, Fig. S7).

The early appearance of serum neutralizing activity following YFV-17D vaccination suggests the presence of nAbs in the PB compartment (*SI Appendix*, Fig. S1 *E* and *G*). To test this directly, we analyzed the neutralizing activities of the PB-derived, YFV-17D binding mAbs in a microtiter neutralization assay at 100 and 10 nM concentrations. Preliminary studies with a panel of control mAbs showed that neutralization half-maximal inhibitory concentrations (IC_{50}s) in this assay were highly comparable to those observed in a classic focus reduction neutralization test assay (*SI Appendix*, Fig. S8*A*). The neutralizing activities of the PB-derived mAbs ranged from complete neutralization at 10 nM to no detectable neutralization at 100 nM (Fig. 1*E*). Notably, a substantially higher fraction of mAbs isolated from day 14 PBs displayed neutralizing activity compared to those isolated from day 10 PBs, which is consistent with the increased serum neutralizing activity on day 14 versus day 10 in both donors (Fig. 1*F* and *SI Appendix*, Fig. S1 *E* and *G*). Furthermore, neutralization titration experiments on the mAbs displaying at least 50% infection inhibition at 100 nM revealed that 9 to 16% of YFV-17D binding mAbs isolated from day 14 PBs displayed medium to high neutralizing activity (IC_{50}s ≤10 nM) (Fig. 1*F* and *SI Appendix*, Fig. S8*B*). Interestingly, sequence analysis showed that 12.5 to 33% of the PB-derived nAbs utilized VH4-4/VL1-51 germline gene pairing, suggesting recognition of a common antigenic site (*SI Appendix*, Fig. S9). Finally, 53% and 20% of the nAbs isolated from donors 1 and 2, respectively, lacked somatic mutations, indicating that YFV-17D nAbs are present in the naïve B cell repertoire (Fig. 1 *E* and *G*). We conclude that YFV-17D vaccination induces PB responses that originate from both naïve and MBCs, and only a minority of these B cells encode Abs that display potent neutralizing activity.

Different B Cell Populations Mediate Early and Late Memory to YFV-17D. To study the MBC response to YFV-17D, we stained purified B cells from each sampling time point with a panel of B cell surface markers (CD19, CD20, CD27, IgM, IgD, CD21, and CD71) and a fluorescently labeled recombinant YFV E protein. The YFV E antigen used for B cell staining was recognized by two well-characterized control mAbs, 4G2 and 5A, providing evidence for proper folding (13) (*SI Appendix*, Fig. S10*A*). YFV E-specific $swIg^+$ MBCs emerged in both donors by days 14 to 28, peaked between days 90 and 180, and slowly declined between days 180 and 360 (Fig. 2 *A* and *B*).

To further dissect the MBC response to YFV-17D, we single-cell-sorted between 100 to 400 YFV E-reactive B cells from both donors at each sampling time point for mAb cloning and characterization. In order to capture the full heterogeneity of the MBC response, we sorted all YFV E-reactive B cells (regardless of surface phenotype) and used index sorting to track the surface markers expressed on each sorted cell (*SI Appendix*, Fig. S10 *B* and *C*). This analysis revealed that YFV E-specific MBC response in both donors was highly heterogenous at all time points (Fig. 2*C*). At the earliest sampling time point, activated naïve B cells and IgM^+CD27^+ MBCs dominated the response in both donors, but these B cell populations waned rapidly over time (Fig. 2 *C* and *D*). By day 90, less than 15% of the YFV E-specific response was comprised of IgM^+CD27^+ MBCs, and by day 360 only about 5% of YFV E-specific B cells belonged to this MBC population (Fig. 2 *C* and *D*). In contrast, the $swIg^+$ MBC population—which was composed of both $CD27^+$ and $CD27^-$ B cells—expanded between day 14 and day 90 and then remained stable throughout the course of the study (Fig. 2 *C* and *D*).

To determine whether the observed hierarchy of IgM^+ and $swIg^+$ MBC populations was unique to YFV-17D vaccination, we also stained longitudinal samples from two Puumala hantavirus (PUUV)-experienced donors with the same panel of B cell markers described above and a fluorescently labeled PUUV envelope protein subunit (Gn) (*SI Appendix*, Fig. S11*A*). Flow cytometric analysis revealed that PUUV Gn-specific IgM^+ memory cells were present during early convalescence but waned rapidly in both donors (*SI Appendix*, Fig. S11*B*). In contrast, $swIg^+$ MBCs appeared early and were maintained at least until day 349 or 237 (the last sampling time points available) in donors 165 and 192, respectively (*SI Appendix*, Fig. S11*B*). Hence, the longevity of IgM^+ and $swIg^+$ MBC responses observed after primary YFV-17D vaccination is highly similar to that observed following primary infection with PUUV.

Interestingly, sequence analysis revealed that over half of the YFV E-specific mAbs isolated from phenotypically naïve ($IgM^+IgD^+CD27^-$) B cells were somatically mutated, suggesting that these B cells are GC-experienced and therefore represent one or more atypical MBC subsets (*SI Appendix*, Fig. S12 *A* and *B*). A comparable proportion of mAbs isolated from $IgM^+IgD^-CD27^-$

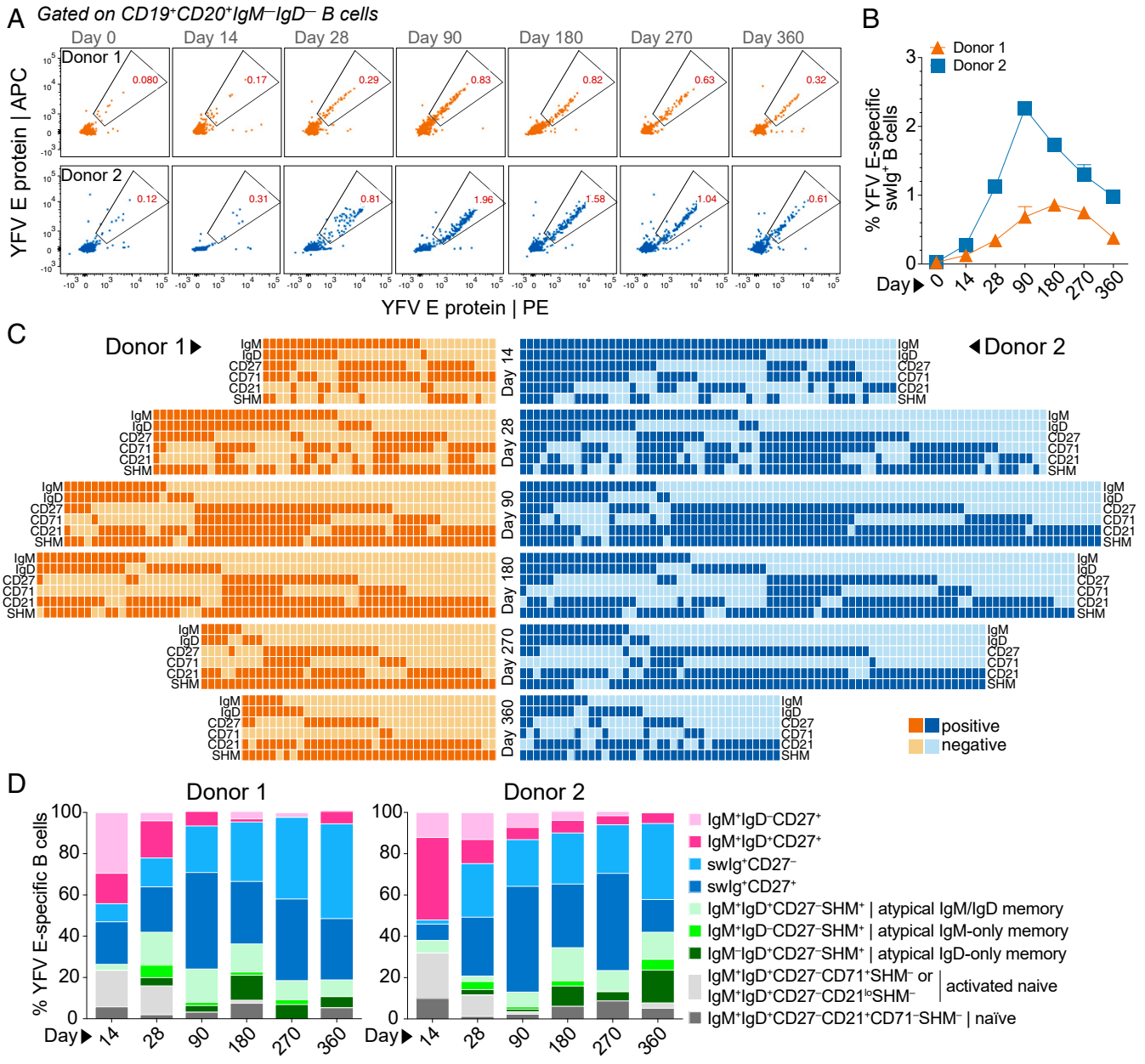

Fig. 2. Different B cell populations mediate early and late memory to YFV-17D. (*A*) Frequency of YFV E-specific swIg$^+$ B cells at each sampling time point. Fluorescence-activated cell sorting plots shown are gated on CD19$^+$CD20$^+$ IgD$^-$ IgM$^-$ B cells. YFV E was labeled with two different colors to reduce background binding. (*B*) Percentage of swIg$^+$ B cells at each sampling time point that display YFV E reactivity. (*C*) Heat map showing the presence or absence of SHM and the indicated B cell surface markers expressed on cells from which YFV E-specific mAbs were isolated. Surface marker expression was determined by flow cytometry. (*D*) Proportion of YFV E-specific B cells at each sampling time point that belong to the indicated B cell subsets.

and IgM$^-$IgD$^+$CD27$^-$ B cells were also somatically mutated, suggesting that these B cells are also bona fide MBCs (*SI Appendix*, Fig. S12 *A* and *B*). The median level of SHM in these three atypical MBC subsets was similar to that observed in classical IgM MBCs (IgM$^+$IgD$^+$CD27$^+$) (*SI Appendix*, Fig. S12*B*). However, in contrast to classical IgM$^+$CD27$^+$ MBCs, these atypical IgM$^+$ and/or IgD$^+$CD27$^-$ MBC populations comprised about one-third of the total YFV E-specific MBC response at day 180 and appeared to be stable until at least day 360 (Fig. 2 *C* and *D*). Overall, the results indicate that the early MBC response to YFV-17D vaccination is mediated by both swIg$^+$ and classical IgM MBCs, whereas the late MBC response is dominated by swIg$^+$ and atypical IgM$^+$ and/or IgD$^+$ MBCs.

Prolonged Evolution of the MBC Response to YFV-17D Vaccination. To characterize the evolution of the MBC response to YFV-17D vaccination, we tracked the SHM loads, apparent binding affinities (K_D^{App}s), and neutralization potencies of the YFV E-specific mAbs at each sampling time point. In both donors, the median level of SHM was low at day 14—with over 50% of Abs lacking somatic mutations—and increased gradually over a 6- to 9-mo time period (Fig. 3 *A* and *B*). By 9 mo postvaccination, SHM loads plateaued in both donors, with a median of nine and seven nucleotide substitutions in V_H for donors 1 and 2, respectively (Fig. 3 *A* and *B*). Consistent with the mutational load analysis, binding studies with a recombinant YFV E protein showed that the K_D^{App}s of the MBC-derived mAbs were very weak at early time points and progressively improved for 6 to 9 mo

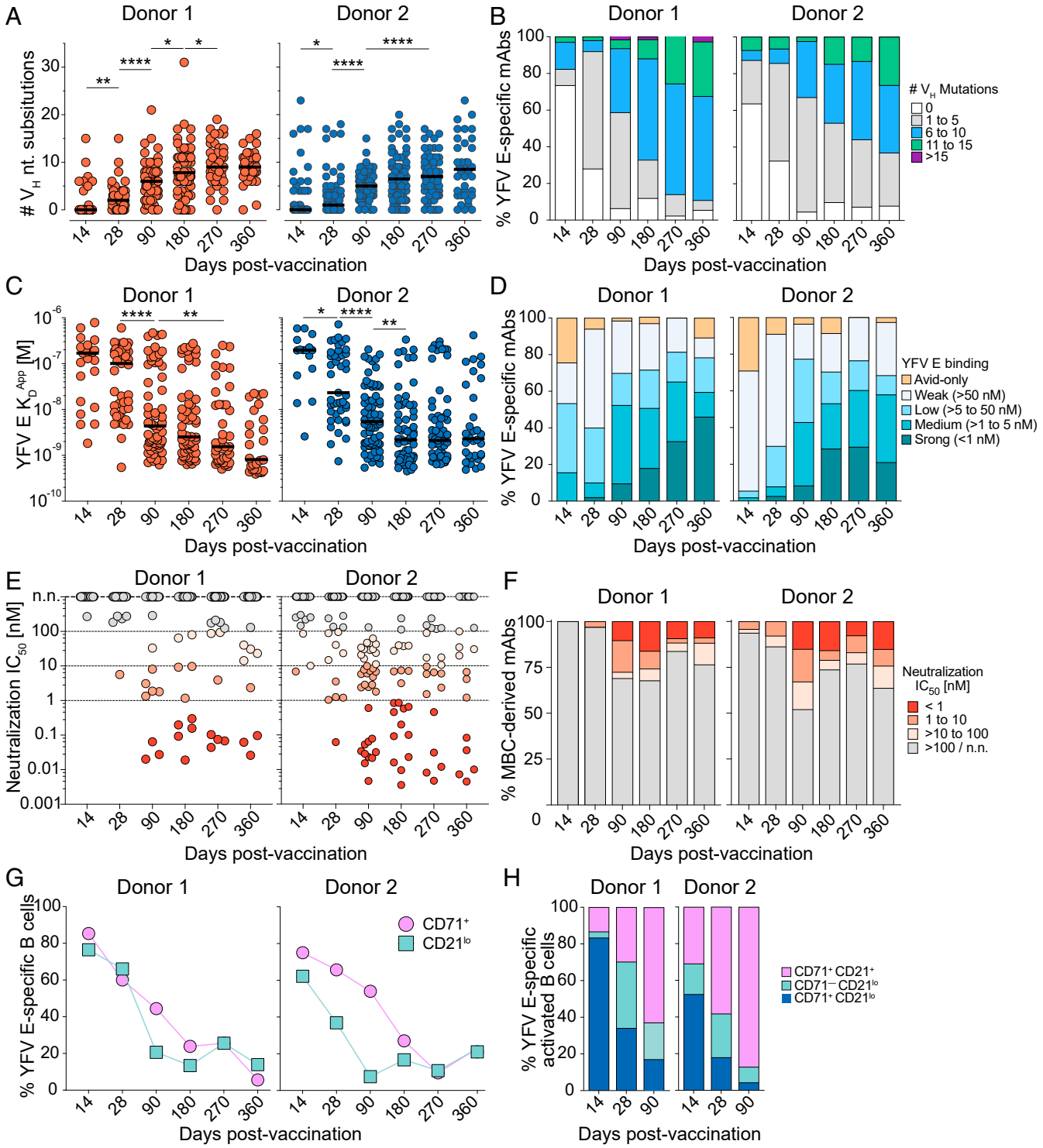

Fig. 3. Ab affinity maturation continues for 6 to 9 mo following YFV-17D vaccination. (*A*) SHM loads of YFV E-specific mAbs isolated from each sampling time point. (*B*) Proportion of YFV E-specific mAbs with the indicated SHM loads. (*C*) K_D^{App}s of the YFV E-specific mAbs isolated at each sampling time point, as determined by BLI. MAbs that did not display detectable binding to the YFV E protein were excluded from this analysis. (*D*) Proportion of YFV E-specific mAbs isolated from each sampling time point with the indicated K_D^{App}s. Avid-only binding indicates mAbs that showed binding to YFV E in an avid orientation but not in a monovalent orientation. (*E*) Neutralization IC_{50}s of individual mAbs against YFV-17D. (*F*) Proportion of MBC-derived mAbs with the indicated neutralization IC_{50}s against YFV-17D. Shading in *E* and *F* is identical. (*G*) Proportion of YFV E-specific B cells that display $CD21^{lo}$ or $CD71^{+}$ surface expression, as determined by index sorting analysis. (*H*) Proportion of YFV E-specific activated B cells that express CD71 ($CD71^{+}$) and/or down-regulate CD21 ($CD21^{lo}$) at days 14, 28, and 90 postvaccination, as determined by index sorting analysis. Statistical comparisons were made using the Mann–Whitney *U* test (****$P < 0.0001$, **$P < 0.01$, *$P < 0.05$). Black bars indicate medians. n.n., nonneutralizing.

following vaccination (Fig. 3 *C* and *D*). In parallel with the increase in affinity, we observed the emergence of highly potent nAbs (IC_{50}s <1 nM) beginning at day 90 (Fig. 3 *E* and *F*). These potent nAbs were derived from multiple MBC subsets, including atypical IgM^+ and/or IgD^+ MBCs (*SI Appendix*, Fig. S13). Interestingly, the average binding avidities and neutralization potencies of the mAbs isolated from day 14 MBCs were lower than those isolated from day 14 PBs, suggesting preferential recruitment of high-affinity nAbs into the PB compartment (Figs. 1*F* and 3*F* and *SI Appendix*, Fig. S14).

Finally, we assessed ongoing B cell activation by analyzing expression of the B cell activation/proliferation marker CD71 on YFV E-specific MBCs (4). This marker was expressed on 75 to 85% YFV E-specific B cells at day 14 and remained elevated for 6 to 9 mo in both donors (Fig. 3*G*). Since down-regulation of CD21 has also been shown to be associated with activation of MBCs following infection or vaccination (4–6), we also monitored CD21 expression on YFV E-specific B cells at each sampling time point. In both donors, YFV E-specific $CD21^{lo}$ cells were highly abundant on days 14 and 28 postvaccination, comprising about 40 to 80% of the YFV E-specific response, and then declined rapidly by day 90 (Fig. 3*G*). At day 14, about 25% of YFV E-specific $CD21^{lo}$ cells expressed IgM BCRs and lacked both CD27 expression and somatic mutations (*SI Appendix*, Fig. S15*A*), suggesting a naïve B cell origin. In contrast, at late time points (day 90 and onward) almost all of the YFV E-specific $CD21^{lo}$ cells contained somatic mutations, supporting a GC origin (*SI Appendix*, Fig. S15*B*). Notably, at day 14 postvaccination, there was a high degree of overlap between the $CD71^+$ and $CD21^{lo}$ populations, with 50 to 80% of YFV E-specific activated B cells (defined as $CD71^+$ and/or

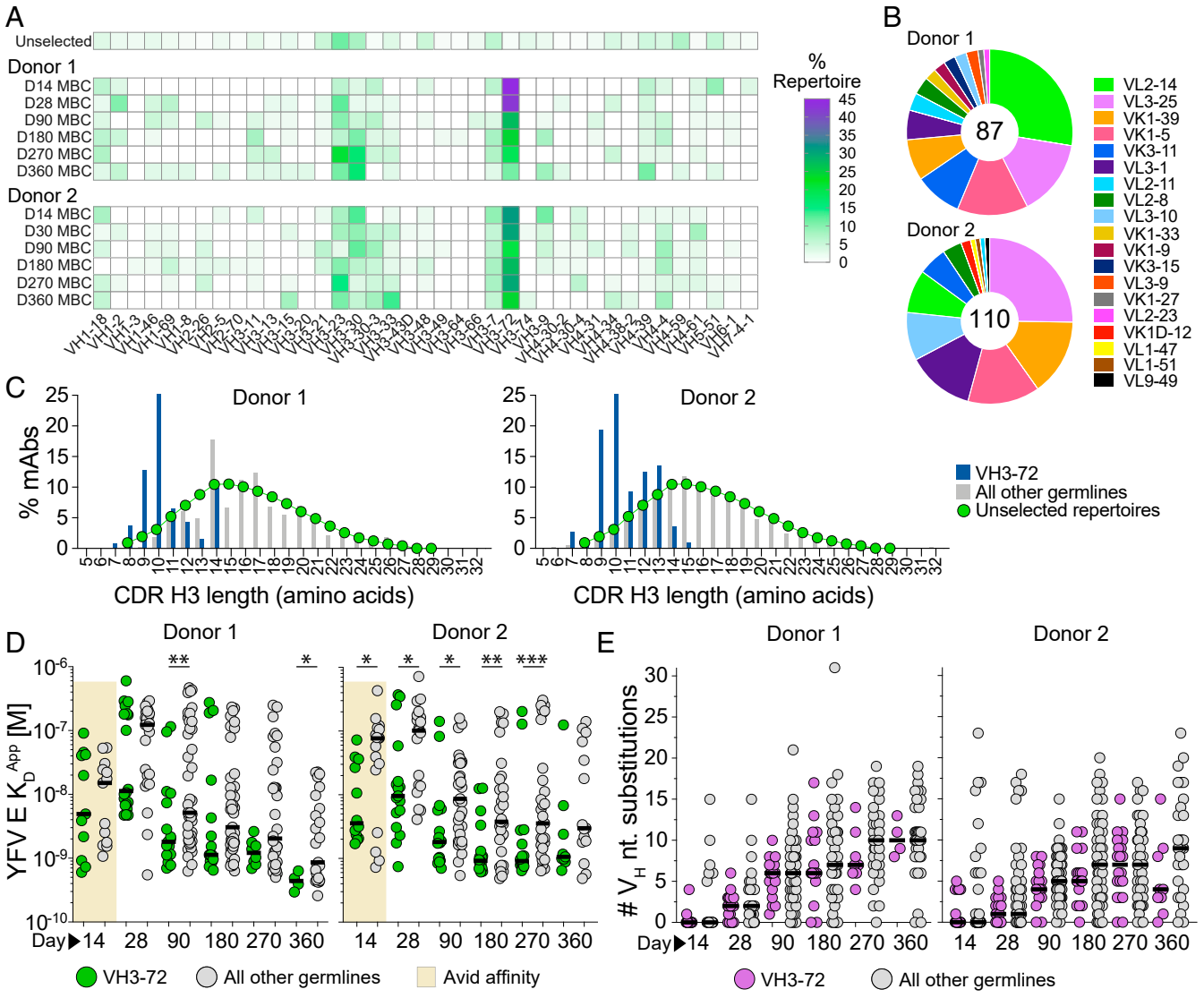

Fig. 4. YFV E-specific mAbs show preferential usage of the VH3-72 germline gene. (*A*) V_H germline gene usage of YFV E-specific mAbs isolated from each sampling time point. V_H germline gene frequencies of unselected human MBCs (Unselected) were obtained from multiple high-throughput sequencing studies and shown for comparison (46). (*B*) V_L germline gene usage of mAbs utilizing the VH3-72 germline gene. The numbers in the center of the pies denote the total number of VH3-72 mAbs. (*C*) CDR H3 length distribution of YFV E-specific mAbs utilizing the VH3-72 germline gene, mAbs utilizing all other V_H germline genes, or unselected Abs from MBCs (46). (*D*) K_D^{App}s of mAbs utilizing the VH3-72 germline gene or all other V_H germline genes, as determined by BLI. Avid K_D^{App}s are plotted for mAbs isolated from day 14 MBCs because only a small subset of these mAbs showed detectable binding to YFV E in a monovalent orientation. (*E*) SHM loads of YFV E-specific mAbs utilizing the VH3-72 germline gene or all other V_H germline genes. Black bars indicate medians. Statistical comparisons were made using the Mann–Whitney *U* test (***$P < 0.001$, **$P < 0.01$, *$P < 0.05$).

CD21^{lo}) displaying a CD71^{+}CD21^{lo} phenotype (Fig. 3*H*). However, by days 28 to 90, the CD71^{+}CD21^{lo} population waned to <20% of the activated B cell response in both donors (Fig. 3*H*). At these time points, the majority of YFV E-specific activated B cells displayed either a CD71^{+}CD21^{+} or CD71^{-}CD21^{lo} phenotype and were heterogenous with respect to isotype and CD27 expression, demonstrating that these B cells belong to multiple distinct MBC populations (Figs. 3*H* and 2*C*). Overall, the results indicate that the YFV E-specific MBC response continues to evolve for 6 to 9 mo following primary vaccination, suggesting that GC activity persists for many months following the period of active viral replication in peripheral blood (22).

The Majority of MBC-Derived mAbs Target Epitopes within or Proximal to the Fusion Loop on DII of the YFV E Protein. We next sought to investigate Ab immunodominance hierarchy in the B cell response to YFV-17D. As a first step, we analyzed the germline gene usage of the isolated mAbs at each sampling time point. Strikingly, in both donors, mAbs utilizing the VH3-72 germline gene dominated the response at all time points (Fig. 4*A*). A large fraction of these mAbs also utilized one of five dominant light-chain germline genes and displayed shorter-than-average heavy-chain complementary determining region 3 (CDRH3) lengths, suggesting a shared mode of antigen recognition (Fig. 4 *B* and *C*). Interestingly, the K_D^{App}s of the mAbs utilizing VH3-72 were significantly lower than those observed for mAbs utilizing other VH germlines, despite containing similar levels of SHM (Fig. 4 *D* and *E*).

To define the number of distinct antigenic sites targeted by the MBC-derived mAbs, we next performed pairwise competition experiments using the newly isolated mAbs and two well-characterized control mAbs, 4G2 and 5A, which recognize proximal but non-overlapping epitopes within DII of the YFV E monomer (Fig. 5*A* and *SI Appendix*, Fig. S16); 4G2 is a pan-flavivirus mAb that targets the fusion loop (FL) (23), whereas 5A is a YFV E-specific mAb that binds to a FL-proximal epitope overlapping the proposed prM association region (Fig. 5*A*) (13). Competition experiments were performed using high-throughput surface plasmon resonance on a Carterra LSA instrument (24). In addition, we tested the mAbs for reactivity with a recombinant YFV-17D DIII protein by BLI.

The majority of mAbs recognized one of eight distinct antigenic sites, which were defined based on reactivity with DIII and competition with 4G2, 5A, and three of the newly isolated mAbs (ADI-49147, ADI-44112, and ADI-45107) (Fig. 5*B* and Dataset S1). Consistent with previous studies of human sera (12), only a small subset of mAbs (6 of 772) recognized epitopes within DIII (Fig. 5*B* and Dataset S1). In contrast, over half of the mAbs from both donors competed with 4G2 and/or 5A, suggesting that the

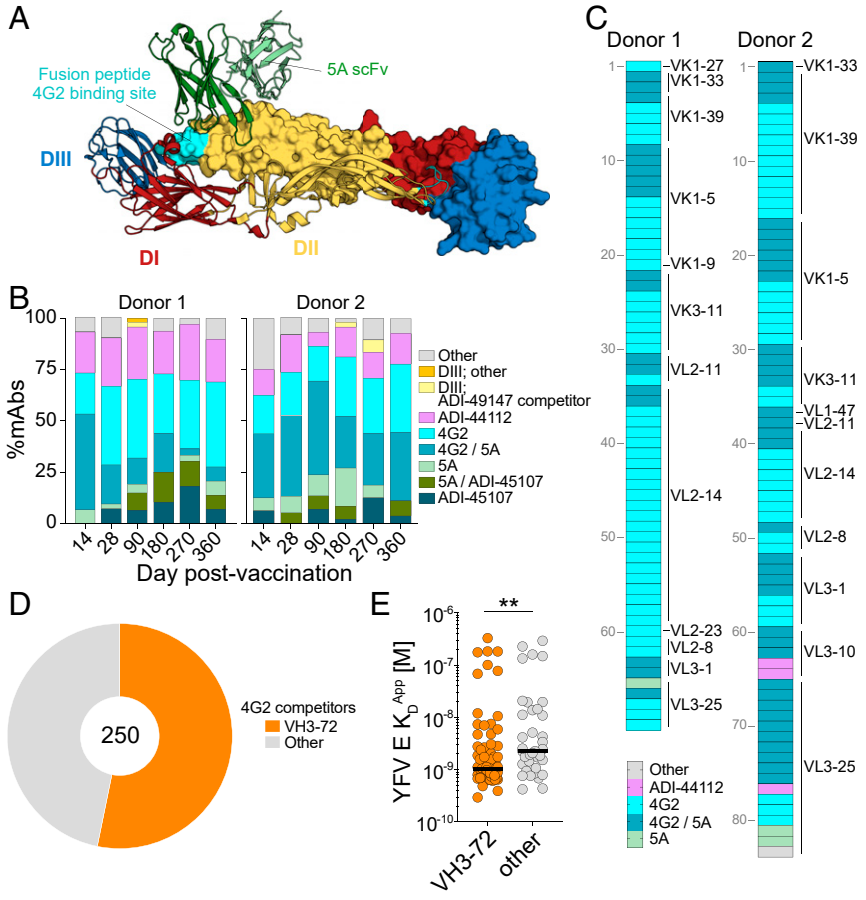

Fig. 5. Abs targeting epitopes within or proximal to the FL dominate the MBC response to YFV-17D vaccination. (*A*) Crystal structure of a soluble YFV E dimer in complex with scFv 5A (13) (Protein Data Bank ID code 6IW2), with the monomers comprising the antiparallel YFV E dimer represented as ribbon or space-filling model. Domains I (red), II (yellow), and III (blue) within the individual monomer unit are colored. The location of the fusion peptide, the site of 4G2 binding, is labeled in cyan (23). (*B*) Proportion of mAbs within each competition group at each sampling time point. (*C*) MAbs utilizing the VH3-72 germline gene are shaded according to their competition group; light-chain germline genes are indicated on the right. (*D*) Proportion of 4G2-competitor mAbs that utilize the VH3-72 germline gene. (*E*) K_D^{App}s of 4G2-competitor mAbs that either use the VH3-72 germline gene or all other germline genes. Statistical comparisons were made using the Mann–Whitney *U* test (**$P < 0.01$). scFv, single-chain variable fragment.

majority of the YFV E-specific response is mediated by Abs that target epitopes within or proximal to the FL on DII (Fig. 5*B*). Interestingly, nearly all of the mAbs that utilized the VH3-72 germline gene competed with 4G2, suggesting recognition of the FL (Fig. 5*C*). Correspondingly, analysis of the sequence features of the mAbs clustered by competition group revealed that over half of the mAbs that competed with 4G2 utilized the VH3-72 germline gene (Fig. 5*D*). Consistent with our previous observation (Fig. 4*E*), the 4G2 competitor mAbs utilizing VH3-72 showed significantly higher affinities compared to those utilizing other V_H germline genes (Fig. 5*E*). Finally, although the proportion of mAbs targeting each antigenic site did not change dramatically over time, we observed a suppression of 4G2/5A competitor mAbs at later time points in donor 1 (days 270 and 360) (Fig. 5*B*). Furthermore, in both donors, mAbs that competed with both 5A and ADI-45107 did not emerge until days 28 to 90 (Fig. 5*B*). Altogether, the results suggest that the vast majority of the YFV E-specific response is directed against epitopes within or proximal to the FL on domain II and that there are only minor shifts in Ab immunodominance hierarchy during the maturation of the B cell response to YFV-17D.

The Majority of Highly Potent nAbs Recognize FL-Proximal Epitopes. We next investigated the relationship between antigenic site and neutralization potency. Strikingly, over 90% of the mAbs that competed either with 5A only or both 5A and ADI-45107 showed neutralizing activity (Fig. 6*A*). Moreover, the majority (78%) of highly potent nAbs (IC_{50} <1 nM) in the panel belonged to these two competition groups (Fig. 6 *B* and *C*). Analysis of the sequence features of 5A-only or 5A/ADI-45107 competitor nAbs revealed that nearly 40% utilized VH4-4/VL1-51 germline gene pairing and did not show evidence of a convergent CDRH3 sequence, suggesting a common mode of germline-encoded antigen recognition (Fig. 6*D* and *SI Appendix*, Table S2). In line with prior studies of other flaviviruses (25), most of the DIII-directed mAbs also showed highly potent neutralizing activity (Fig. 6 *A* and *B*). In contrast to the 5A competitors and DIII-directed mAbs, only a minority of the mAbs belonging to other competition groups showed neutralizing activity (Fig. 6 *A* and *B*). For example, only 12% and 20% of mAbs that competed with 4G2 only or both 4G2 and 5A, respectively, displayed neutralization IC_{50}s <100 nM (Fig. 6 *A* and *B*). Overall, the results demonstrate that, in these two donors, the nAb response to YFV-17D is primarily mediated by Abs that recognize FL-proximal epitopes within DII of the YFV E protein.

A Subset of mAbs Display Binding Cross-Reactivity with Other Flavivirus E Proteins. Since human flavivirus infections are known to induce flavivirus cross-reactive Ab responses (26–28), we next evaluated whether any of the isolated mAbs displayed binding reactivity to recombinant DENV-2, DENV-4, WNV, or ZIKV E proteins. In both donors, about 6% of YFV E-reactive mAbs showed cross-reactivity to at least one heterologous flavivirus E protein (Fig. 7*A*). The majority of these cross-reactive mAbs targeted the highly conserved FL and bound to all five flavivirus E proteins with high apparent affinities (K_D^{App}s <10 nM) (Fig. 7 *B* and *C*). Correspondingly, the small subset of mAbs that bound to epitopes outside of the FL generally displayed more limited cross-reactivity profiles and lower affinities (Fig. 7*C*). Importantly, only 6 out of 50 cross-binding mAbs showed neutralizing activity against YFV-17D, and none of these mAbs showed significant cross-neutralizing activity against ZIKV, WNV, or JEV (Fig. 7 and *SI Appendix*, Fig. S17). We conclude that YFV-17D vaccination induces a subset of Abs that display broad flavivirus binding activity, the majority of which target the highly conserved FL and show little to no cross-neutralizing activity.

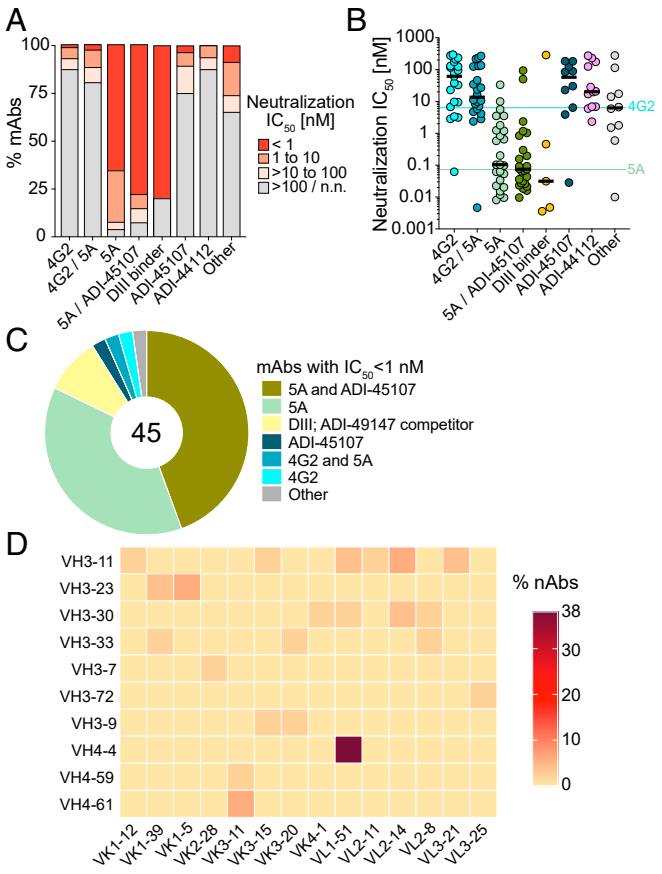

Fig. 6. The majority of highly potent nAbs recognize FL-proximal epitopes. (*A*) Proportion of mAbs in each competition group with the indicated neutralization IC_{50}s against YFV-17D. (*B*) Neutralization IC_{50}s of individual mAbs against YFV-17D across the indicated competition groups. Black bars indicate medians. IC_{50} values for 4G2 and 5A mAbs are indicated by horizontal lines. (*C*) Antigenic sites targeted by highly potent nAbs (IC_{50} <1 nM). The number in the center of the pie indicates the total number of highly potent nAbs. (*D*) V_H and V_L germline gene usage of 5A-only and 5A/ADI-45107 competitor nAbs.

Discussion

A deep understanding of the kinetics, dynamics, and specificities of human MBC responses elicited by successful vaccines may provide insights into the design of vaccines for refractory pathogens. To dissect the antigen-specific MBC response induced by the YFV-17D vaccine—widely considered to be the "gold-standard" of antiviral vaccination—we cloned and characterized hundreds of YFV E-specific mAbs from two healthy donors at multiple time points following primary YFV-17D vaccination.

In most individuals, YFV serum neutralizing activity appears ~10 to 14 d following primary YFV-17D vaccination (29, 30), which corresponds to the peak PB response and suggests the presence of nAbs in this compartment. Indeed, we found that about one-third of the YFV E-specific mAbs isolated from day 14 PBs showed neutralizing activity. The PB-derived nAbs originated from both mutated and unmutated cells, suggesting that both activated naïve and MBCs contribute to the nAb response to YFV-17D. Interestingly, the average binding avidities and neutralization potencies of the mAbs isolated from day 14 PBs were higher than those isolated from day 14 MBCs, which is consistent with previous studies in mouse models showing that higher-affinity cells are preferentially recruited into the PB compartment (31, 32). Hence, the immune system appears to place a priority on the rapid production of high-affinity serum

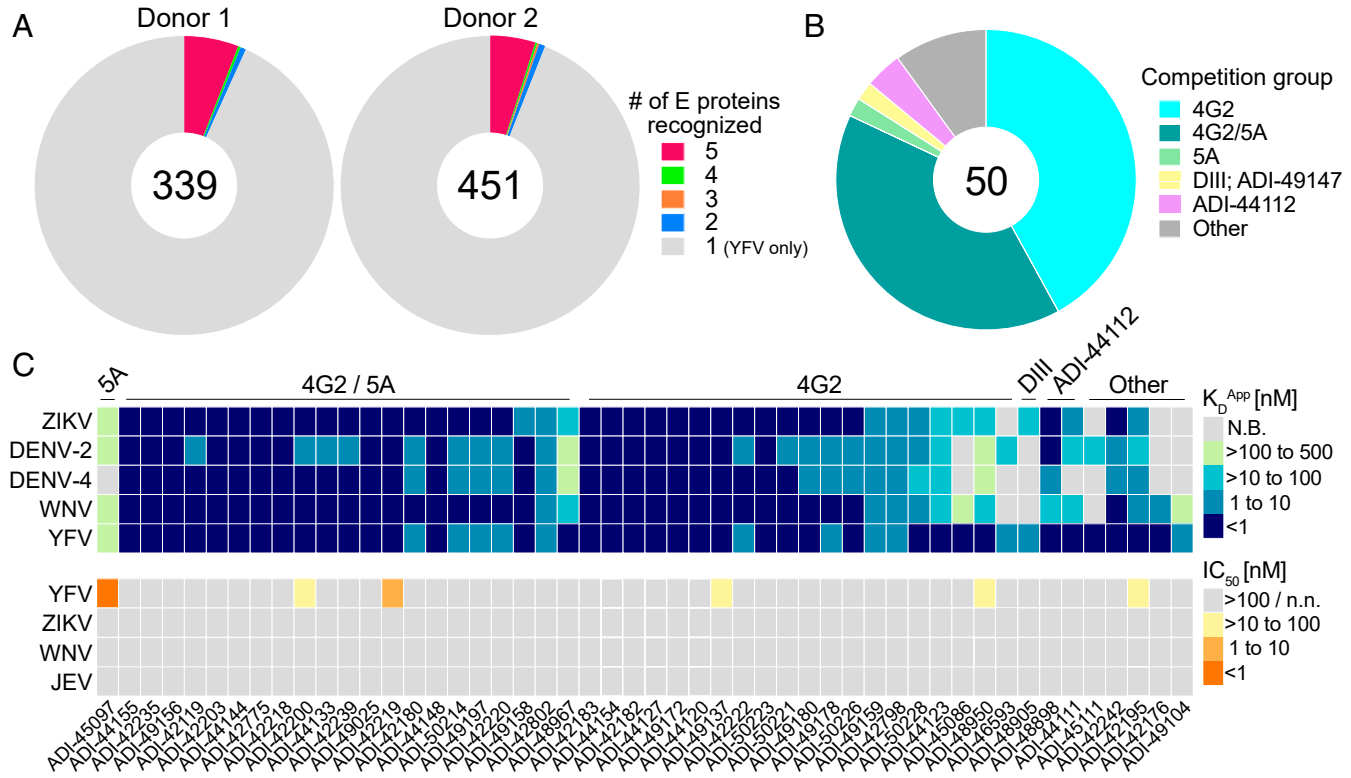

Fig. 7. A subset of mAbs show broad flavivirus cross-reactivity. (*A*) Proportion of mAbs that react with one or more of the flavivirus E proteins tested (YFV, DENV-1, DENV-2, ZIKV, and WNV). Numbers in the center of the pies indicate the number of mAbs analyzed. (*B*) Proportion of cross-reactive mAbs that recognize the indicated antigenic sites. (*C*, *Top*) Heat map shows the binding cross-reactivity profiles of 50 mAbs that showed binding reactivity to at least one flavivirus E protein in addition to YFV E. (*C*, *Bottom*) Heat map shows the neutralizing activities of the cross-binding mAbs against YFV-17D, ZIKV, WNV, and JEV. Competition group assignments for the individual mAbs are indicated at the top of the heat map. N.B., nonbinding; n.n., nonneutralizing.

nAbs, which likely provides the basis for the early protection afforded by the YFV-17D vaccine.

Previous studies in mouse models have demonstrated that antigen-specific IgM^+ MBCs are induced early after immunization and remain numerically stable over time (8–10). In contrast, the longevity of $swIg^+$ MBCs has been suggested to be dependent on the frequency of high-affinity germline-encoded precursors in the naïve B cell repertoire, with the presence of high-affinity naïve precursors associated with unstable $swIg^+$ MBCs (8, 9). Interestingly, despite the presence of germline-encoded BCRs with high avidity for YFV E in both donors, we observed that classical IgM^+ MBCs waned rapidly over time, whereas $swIg^+$ MBCs remained stable until at least day 360 postvaccination. Although the results from these two vaccinated donors may not be representative of the entire YFV-17D–vaccinated population, we also observed transient IgM^+ MBCs and long-lived $swIg^+$ MBCs in the context of PUUV infection and others have reported long-term maintenance of $swIg^+$ MBCs following smallpox vaccination (33), suggesting that primary viral infections commonly induce a stable $swIg^+$ MBC population. The discrepancy between our results and those observed in mouse models may reflect differences between the hierarchy of IgM^+ versus $swIg^+$ MBC response in mice and humans and/or differences in the response to replicating versus nonreplicating antigens.

We observed increases in SHM, Ab affinity, and neutralization potency for 6 to 9 mo following YFV-17D vaccination, suggesting that GC activity continues for many months following the period of detectable viral replication in peripheral blood. This could either be due to low level viral replication in secondary lymphoid organs or prolonged capture of inert viral antigens on the surface of follicular dendritic cells (FDCs). Although we cannot distinguish between these two possibilities, previous studies have shown that viral antigens, in the form of complement-coated immune complexes, can be sequestered by FDCs for extended periods of time for presentation to GC B cells (34–37). Importantly, recent studies have also shown that MBCs induced by Ebola virus infection and influenza virus vaccination continue to undergo affinity maturation for 6 to 12 mo (6, 38, 39), suggesting that prolonged maturation of the MBC response may be more common than previously appreciated. Given that Ab responses induced by live viral infections have been shown to have half-lives of 50 y or more, whereas responses to nonreplicating protein antigens wane relatively quickly and require booster vaccinations (40), it will be of interest to investigate whether protracted affinity maturation is also observed for vaccines that do not induce long-lived Ab responses (e.g., the tetanus toxoid and diphtheria vaccines).

In both donors the nAb response induced by YFV-17D vaccination was primarily directed against FL-proximal epitopes overlapping the 5A binding site. Interestingly, a substantial fraction of these "5A-class" nAbs displayed convergent V_H/V_L germline gene pairing, suggestive of a so-called public Ab response (41). The relatively high abundance of these two germline genes (VH4-4 and VL1-51) in the naïve B cell repertoire perhaps provides a molecular explanation for how the YFV-17D vaccine is able to induce protective neutralizing Ab responses in such an extraordinarily high proportion of individuals (>95%) (42, 43). Furthermore, a subset of these nAbs displayed exceptionally potent neutralizing activity, with IC_{50}s that were about 10 times lower than previously described YFV mAbs (13, 14). Given the recent YFV outbreaks in Brazil and the Democratic Republic of

Congo, coupled with YFV-17D vaccine supply shortages and the lack of effective treatments for YFV disease, these mAbs represent promising candidates for prophylaxis and/or therapy.

Interestingly, about 6% of Abs induced by YFV-17D vaccination showed binding reactivity to heterologous flavivirus E proteins. As expected based on prior studies of flavivirus infection (26–28), we found that the majority of these mAbs targeted the highly conserved FL and lacked measurable cross-neutralizing activity. Although nonneutralizing Abs are unlikely to contribute to protection or Ab-dependent enhancement of secondary flavivirus infections (44), the corresponding cross-reactive B cells may be preferentially activated and expanded upon subsequent flavivirus infection. Thus, it will be of interest to study if and how preexisting YFV immunity impacts the B cell response to heterologous flavivirus exposure and vice versa.

Altogether, the results of this study provide a comprehensive view of the dynamics and complexity of the human MBC response induced by the highly successful YFV-17D vaccine. Similar studies performed on other vaccines and natural infections may shed light on features of the MBC response associated with the induction and maintenance of long-term protective Ab responses.

Materials and Methods

Human Subjects. Informed consent to participate in this study was obtained before vaccination. Study subjects aged between 25 and 32 y were vaccinated with the YFV-17D Stamaril vaccine. Heparinized blood (50 to 100 cc) was obtained from subjects before vaccination and on days 10, 14, 28, 90, 180, 270, and 360 following vaccination. Samples were processed in the Immune Monitoring and Flow Cytometry Core laboratory at the Geisel School of Medicine at Dartmouth College to obtain plasma and to isolate peripheral blood-derived B cells. Isolated cells and plasma were stored frozen in aliquots at −80 °C. This study complies with all relevant ethical regulations for work with human participants and was approved by the Committee for the Protection of Human Subjects, Dartmouth-Hitchcock Medical Center, and Dartmouth College.

Blood samples from the two PUUV-experienced donors were obtained on days 20, 35, 82, 130, 161, 237, and 349 postdiagnosis. Both donors were hospitalized due to PUUV-associated disease. Samples were processed at the University Hospital of Northern Sweden to obtain plasma and to isolate peripheral blood-derived B cells. The two subjects were 43 (donor 165) and 75 (donor 192) y of age at the time of hospitalization. Ethical approval was obtained by the regional Ethical Review Board at Umeå University, Umeå, Sweden. Signed informed consent was obtained from both donors.

Single B Cell Sorting and Variable Gene Amplification. MBCs were stained using anti-human CD19, CD20, CD3, CD8, CD14, CD16, IgD, IgM, CD27, CD21, CD71, and a mixture of dual-labeled (APC and PE) YFV E tetramers. B cells that showed reactivity to the YFV E tetramers were single-cell-sorted for mAb cloning, as described previously (45).

Microtiter Neutralization Assays. Monoclonal antibodies were serially diluted in cell culture medium and incubated at room temperature with the test viruses (YFV-17D or ZIKV) or test reporter virus particles (RVPs) (WNV or JEV) for 1 h then added to cells. Infection levels were measured 2 d later by staining infected cells with the pan-flavivirus mouse mAb 4G2 on a Cytation-5 automated fluorescence microscope (BioTek).

Data Availability. All data are included in the manuscript and *SI Appendix*. All reagent and data requests should be directed to L.M.W. The sequences of neutralizing antibodies isolated in this study have been deposited in the GenBank database, https://www.ncbi.nlm.nih.gov/genbank (accession nos. MN993290–MN993593).

ACKNOWLEDGMENTS. We thank Dr. Ted Pierson for his generous gift of the flavivirus RVP system and Alan Bergeron from the Dartmouth Immune Monitoring and Flow Cytometry Core laboratory for carrying out human peripheral blood mononuclear cell processing and banking. This work was supported by the NIH grant NIAID R01 AI134824 (to K.C.) and by the transnational Agence Nationale de la Recherche/Deutsche Forschungsgemeinschaft grant FlavImmunity/ANR-17-CE15-0031-01 (to G.B.-S.).

1. L. Mesin, J. Ersching, G. D. Victora, Germinal center B cell dynamics. *Immunity* **45**, 471–482 (2016).
2. F. Weisel, M. Shlomchik, Memory B cells of mice and humans. *Annu. Rev. Immunol.* **35**, 255–284 (2017).
3. J. J. Taylor, M. K. Jenkins, K. A. Pape, Heterogeneity in the differentiation and function of memory B cells. *Trends Immunol.* **33**, 590–597 (2012).
4. A. H. Ellebedy *et al*., Defining antigen-specific plasmablast and memory B cell subsets in human blood after viral infection or vaccination. *Nat. Immunol.* **17**, 1226–1234 (2016).
5. D. Lau *et al*., Low CD21 expression defines a population of recent germinal center graduates primed for plasma cell differentiation. *Sci. Immunol.* **2**, eaai8153 (2017).
6. S. F. Andrews *et al*., Activation dynamics and immunoglobulin evolution of pre-existing and newly generated human memory B cell responses to influenza hemagglutinin. *Immunity* **51**, 398–410.e5 (2019).
7. G. V. Zuccarino-Catania *et al*., CD80 and PD-L2 define functionally distinct memory B cell subsets that are independent of antibody isotype. *Nat. Immunol.* **15**, 631–637 (2014).
8. K. A. Pape *et al*., Naive B cells with high-avidity germline-encoded antigen receptors produce persistent IgM(+) and transient IgG(+) memory B cells. *Immunity* **48**, 1135–1143 e4 (2018).
9. K. A. Pape, J. J. Taylor, R. W. Maul, P. J. Gearhart, M. K. Jenkins, Different B cell populations mediate early and late memory during an endogenous immune response. *Science* **331**, 1203–1207 (2011).
10. I. Dogan *et al*., Multiple layers of B cell memory with different effector functions. *Nat. Immunol.* **10**, 1292–1299 (2009).
11. R. A. Mason, N. M. Tauraso, R. O. Spertzel, R. K. Ginn, Yellow fever vaccine: Direct challenge of monkeys given graded doses of 17D vaccine. *Appl. Microbiol.* **25**, 539–544 (1973).
12. O. Vratskikh *et al*., Dissection of antibody specificities induced by yellow fever vaccination. *PLoS Pathog.* **9**, e1003458 (2013).
13. X. Lu *et al*., Double lock of a human neutralizing and protective monoclonal antibody targeting the yellow fever virus envelope. *Cell Rep.* **26**, 438–446 e5 (2019).
14. S. Daffis *et al*., Antibody responses against wild-type yellow fever virus and the 17D vaccine strain: Characterization with human monoclonal antibody fragments and neutralization escape variants. *Virology* **337**, 262–272 (2005).
15. R. W. Wieten *et al*., A single 17D yellow fever vaccination provides lifelong immunity; characterization of yellow-fever-specific neutralizing antibody and T-cell responses after vaccination. *PLoS One* **11**, e0149871 (2016).
16. N. P. Lindsey *et al*., Persistence of yellow fever virus-specific neutralizing antibodies after vaccination among US travellers. *J. Travel Med.* **25**, tay108 (2018).
17. S. Kohler *et al*., The early cellular signatures of protective immunity induced by live viral vaccination. *Eur. J. Immunol.* **42**, 2363–2373 (2012).
18. M. S. Gilman *et al*., Rapid profiling of RSV antibody repertoires from the memory B cells of naturally infected adult donors. *Sci. Immunol.* **1**, eaaj1879 (2016).
19. R. Di Niro *et al*., Salmonella infection drives promiscuous B cell activation followed by extrafollicular affinity maturation. *Immunity* **43**, 120–131 (2015).
20. W. Dejnirattisai *et al*., A new class of highly potent, broadly neutralizing antibodies isolated from viremic patients infected with dengue virus. *Nat. Immunol.* **16**, 170–177 (2015).
21. J. Wrammert *et al*., Rapid cloning of high-affinity human monoclonal antibodies against influenza virus. *Nature* **453**, 667–671 (2008).
22. B. Reinhardt, R. Jaspert, M. Niedrig, C. Kostner, J. L'age-Stehr, Development of viremia and humoral and cellular parameters of immune activation after vaccination with yellow fever virus strain 17D: A model of human flavivirus infection. *J. Med. Virol.* **56**, 159–167 (1998).
23. W. D. Crill, G. J. Chang, Localization and characterization of flavivirus envelope glycoprotein cross-reactive epitopes. *J. Virol.* **78**, 13975–13986 (2004).
24. A. Sivasubramanian *et al*., Broad epitope coverage of a human in vitro antibody library. *MAbs* **9**, 29–42 (2017).
25. E. N. Gallichotte *et al*., Role of Zika virus envelope protein domain III as a target of human neutralizing antibodies. *MBio* **10**, e01485-19 (2019).
26. C. H. Calisher *et al*., Antigenic relationships between flaviviruses as determined by cross-neutralization tests with polyclonal antisera. *J. Gen. Virol.* **70**, 37–43 (1989).
27. K. L. Mansfield *et al*., Flavivirus-induced antibody cross-reactivity. *J. Gen. Virol.* **92**, 2821–2829 (2011).
28. L. Priyamvada *et al*., Human antibody responses after dengue virus infection are highly cross-reactive to Zika virus. *Proc. Natl. Acad. Sci. U.S.A.* **113**, 7852–7857 (2016).
29. T. P. Monath *et al*., Comparative safety and immunogenicity of two yellow fever 17D vaccines (ARILVAX and YF-VAX) in a phase III multicenter, double-blind clinical trial. *Am. J. Trop. Med. Hyg.* **66**, 533–541 (2002).
30. J. Lang *et al*., Comparison of the immunogenicity and safety of two 17D yellow fever vaccines. *Am. J. Trop. Med. Hyg.* **60**, 1045–1050 (1999).
31. J. J. Taylor, K. A. Pape, H. R. Steach, M. K. Jenkins, Humoral immunity. Apoptosis and antigen affinity limit effector cell differentiation of a single naïve B cell. *Science* **347**, 784–787 (2015).
32. D. Paus *et al*., Antigen recognition strength regulates the choice between extrafollicular plasma cell and germinal center B cell differentiation. *J. Exp. Med.* **203**, 1081–1091 (2006).
33. S. Crotty *et al*., Cutting edge: Long-term B cell memory in humans after smallpox vaccination. *J. Immunol.* **171**, 4969–4973 (2003).

34. B. A. Heesters *et al*., Endocytosis and recycling of immune complexes by follicular dendritic cells enhances B cell antigen binding and activation. *Immunity* **38**, 1164–1175 (2013).
35. B. A. Smith *et al*., Persistence of infectious HIV on follicular dendritic cells. *J. Immunol.* **166**, 690–696 (2001).
36. B. A. Heesters, R. C. Myers, M. C. Carroll, Follicular dendritic cells: Dynamic antigen libraries. *Nat. Rev. Immunol.* **14**, 495–504 (2014).
37. J. G. Tew, T. E. Mandel, Prolonged antigen half-life in the lymphoid follicles of specifically immunized mice. *Immunology* **37**, 69–76 (1979).
38. C. W. Davis *et al*., Longitudinal analysis of the human B cell response to Ebola virus infection. *Cell* **177**, 1566–1582 e17 (2019).
39. K. Matsuda *et al*, Prolonged evolution of the memory B cell response induced by a replicating adenovirus-influenza H5 vaccine. *Sci. Immunol.* **4**, eaau2710 (2019).
40. I. J. Amanna, N. E. Carlson, M. K. Slifka, Duration of humoral immunity to common viral and vaccine antigens. *N. Engl. J. Med.* **357**, 1903–1915 (2007).
41. A. Lanzavecchia, Dissecting human antibody responses: Useful, basic and surprising findings. *EMBO Mol. Med.* **10**, e8879 (2018).
42. B. Briney, A. Inderbitzin, C. Joyce, D. R. Burton, Commonality despite exceptional diversity in the baseline human antibody repertoire. *Nature* **566**, 393–397 (2019).
43. N. D. Collins, A. D. Barrett, Live attenuated yellow fever 17D vaccine: A legacy vaccine still controlling outbreaks in modern day. *Curr. Infect. Dis. Rep.* **19**, 14 (2017).
44. M. J. Luppe *et al*., Yellow fever (YF) vaccination does not increase dengue severity: A retrospective study based on 11,448 dengue notifications in a YF and dengue endemic region. *Travel Med. Infect. Dis.* **30**, 25–31 (2019).
45. T. Tiller *et al*., Efficient generation of monoclonal antibodies from single human B cells by single cell RT-PCR and expression vector cloning. *J. Immunol. Methods* **329**, 112–124 (2008).
46. A. Kovaltsuk *et al*., Observed antibody space: A resource for data mining next-generation sequencing of antibody repertoires. *J. Immunol.* **201**, 2502–2509 (2018).